blood advances

American Society of Hematology
2021 L Street NW, Suite 900,
Washington, DC 20036
Phone: 202-776-0544 | Fax 202-776-0545
bloodadvances@hematology.org

RUNX1 C-terminal Mutations Impair Blood Cell Differentiation by Perturbing Specific Enhancer-Promoter Networks

Tracking no: ADV-2023-011484R1

Nathan Jayne (University of California San Diego, United States) Zhengyu Liang (University of California San Diego, United States) Do-Hwan Lim (University of California San Diego, United States) Poshen Chen (University of California San Diego, United States) Cristina Diaz (University of California San Diego, United States) Kei-Ichiro Arimoto (University of California San Diego, United States) Lingbo Xia (University of California San Diego, United States) Mengdan Liu (University of California San Diego, United States) Bing Ren (University of California San Diego, United States) Xiang-Dong Fu (Westlake University, China) Dong-Er Zhang (University of California San Diego, United States)

Abstract:
The transcription factor RUNX1 is a master regulator of hematopoiesis and is frequently mutated in myeloid malignancies. Mutations in its runt homology domain (RHD) frequently disrupt DNA binding and result in loss of RUNX1 function. However, it is not clearly understood how other RUNX1 mutations contribute to disease development. Here, we characterize RUNX1 mutations outside of the RHD. Our analysis of patient datasets revealed that mutations within the C-terminus frequently occur in hematopoietic disorders. Remarkably, most of these mutations were nonsense or frameshift and predicted to be exempt from nonsense mediated mRNA decay. Therefore, this class of mutation is projected to produce DNA-binding proteins that contribute to pathogenesis in a distinct manner. To model this, we introduced the RUNX1R320* mutation into the endogenous gene locus and demonstrated the production of RUNX1R320* protein. Expression of RUNX1R320* resulted in the disruption of RUNX1 regulated processes such as megakaryocytic differentiation through a transcriptional signature different from RUNX1 depletion. To understand the underlying mechanisms, we utilized Global RNA Interactions with DNA by deep sequencing (GRID-seq) to examine enhancer-promoter connections. We identified wide-spread alteration of enhancer-promoter networks within RUNX1 mutant cells. Additionally, we uncovered enrichment of RUNX1R320* and FOXK2 binding at the MYC super enhancer locus, significantly upregulating MYC transcription and signaling pathways. Together, our study demonstrates that most RUNX1 mutations outside the DNA binding domain are not subject to nonsense mediated decay, producing protein products that act in concert with additional cofactors to dysregulate hematopoiesis through mechanisms distinct from that induced by RUNX1 depletion.

Conflict of interest: COI declared - see note

COI notes: B.R. is a cofounder of Epigenome Technologies, Inc. and has equity in Arima Genomics, Inc.

Preprint server: No;

Author contributions and disclosures: Contribution: N.D.J. and D.-E.Z. devised the study and designed the experimental strategies; N.D.J. performed the research, collected the data, and analyzed the results; D.-H.L. and P.B.C. prepared the GRID-seq and ChIP-seq libraries respectively; Z.L. performed bioinformatic analyses pertaining to GRID-seq datasets; C.D. and L.X. performed microscopy-based data collection and analysis. K.-I.A. assisted in protein expression/interaction experiments. M.L. assisted in flow cytometry experiments and related statistical analysis. N.D.J. wrote the manuscript; X.-D.F., and B.R. provided resources, imparted expertise, and critically reviewed the manuscript; and D.-E.Z. oversaw the study, supervised manuscript preparation, and secured funding to support the study.

Non-author contributions and disclosures: No;

Agreement to Share Publication-Related Data and Data Sharing Statement: All RNA-seq, ChIP-seq, and GRID-seq data have been deposited in the Gene Expression Omnibus database under GSE236641, GSE236638, and GSE236640, respectively.

Clinical trial registration information (if any):

RUNX1 C-terminal Mutations Impair Blood Cell Differentiation by Perturbing Specific Enhancer-Promoter Networks

Running Head: RUNX1 Truncation Alters Enhancer Promoter Networks

Nathan D. Jayne[1,2], Zhengyu Liang[3†], Do-Hwan Lim[3‡], Poshen B. Chen[3§], Cristina Diaz[1,2], Kei-Ichiro Arimoto[1], Lingbo Xia[1,2], Mengdan Liu[1,2], Bing Ren[3], Xiang-Dong Fu[4], Dong-Er Zhang[1,2,3]

[1] Moores UCSD Cancer Center, University of California San Diego, La Jolla, CA
[2] School of Biological Sciences, University of California San Diego, La Jolla, CA
[3] School of Medicine, University of California, San Diego, La Jolla, CA
[4] School of Life Sciences, Westlake University, Hangzhou, Zhejiang, China

Corresponding Author: Dong-Er Zhang, d7zhang@health.ucsd.edu 9500 Gilman Dr #0815, La Jolla, CA 92037 Phone: (858) 822-5372 Fax (858) 822-5433

Current affiliations:

[†] School of Life Sciences, Southern University of Science and Technology, Shenzhen, Guangdong, China
[‡] School of Systems Biomedical Science, Soongsil University, Seoul 06978, Republic of Korea
[§] Genome Institute of Singapore, Agency for Science, Technology and Research (A*STAR), Singapore 138672, Singapore

Data Sharing Statement

All RNA-seq, ChIP-seq, and GRID-seq data have been deposited in the Gene Expression Omnibus database under GSE236641, GSE236638, and GSE236640, respectively.

Key Points

- Most RUNX1 mutations outside the RHD are nonsense and frameshift and produce proteins lacking critical RUNX1 regulatory domains
- The truncation of RUNX1 results in dysregulation of hematopoietic and oncogenic pathways through changes in enhancer-promoter networks

Full Text: 3947

Abstract: 250

Figures: 6

References: 76

Abstract

The transcription factor RUNX1 is a master regulator of hematopoiesis and is frequently mutated in myeloid malignancies. Mutations in its runt homology domain (RHD) frequently disrupt DNA binding and result in loss of RUNX1 function. However, it is not clearly understood how other RUNX1 mutations contribute to disease development. Here, we characterize RUNX1 mutations outside of the RHD. Our analysis of patient datasets revealed that mutations within the C-terminus frequently occur in hematopoietic disorders. Remarkably, most of these mutations were nonsense or frameshift and predicted to be exempt from nonsense mediated mRNA decay. Therefore, this class of mutation is projected to produce DNA-binding proteins that contribute to pathogenesis in a distinct manner. To model this, we introduced the RUNX1^{R320*} mutation into the endogenous gene locus and demonstrated the production of RUNX1^{R320*} protein. Expression of RUNX1^{R320*} resulted in the disruption of RUNX1 regulated processes such as megakaryocytic differentiation through a transcriptional signature different from RUNX1 depletion. To understand the underlying mechanisms, we utilized Global RNA Interactions with DNA by deep sequencing (GRID-seq) to examine enhancer-promoter connections. We identified wide-spread alteration of enhancer-promoter networks within RUNX1 mutant cells. Additionally, we uncovered enrichment of RUNX1^{R320*} and FOXK2 binding at the MYC super enhancer locus, significantly upregulating MYC transcription and signaling pathways. Together, our study demonstrates that most RUNX1 mutations outside the DNA binding domain are not subject to nonsense mediated decay, producing protein products that act in concert with additional cofactors to dysregulate hematopoiesis through mechanisms distinct from that induced by RUNX1 depletion.

Introduction

Hematopoiesis is a vastly complex process, involving many signaling pathways, intricate transcriptional programs, in addition to further epigenetic and RNA splicing regulation. At the top

of the hematopoietic hierarchy lie several master regulators which play critical roles throughout the proliferation and differentiation process. RUNX1 is among these master regulators and is required for definitive hematopoiesis[1–4].

Pathogenic mutations occur throughout RUNX1. Many mutations have been detected within the DNA-binding Runt homology domain (RHD) which disrupt protein binding to DNA and act as loss-of-function mutations. Outside of the RHD, mutations affect the regulatory regions located in the C-terminus of RUNX1[5–7]. These mutations have been associated with sporadic MDS/AML[8,9], increased risk of AML transformation in CMML patients[10]. Germline mutations in this region have also been identified as pathogenic drivers in familial platelet disorder with associated myeloid malignancy (FPDMM)[11–13].

Although C-terminal mutations in RUNX1 have been proven to be pathogenic, the underlying mechanisms of this class of mutation remain poorly understood in hematopoietic disorders. We revealed that the majority of C-terminal mutations are nonsense and frameshift mutations that are exempt from nonsense mediated mRNA decay (NMD). Furthermore, to understand the mechanisms and impacts of these C-terminal mutations, we generated an isogenic knock-in human cell line model of RUNX1^{R320*} (RUNX1c notation is used in this study)[13,14]. Our studies established that RUNX1^{R320*} does not elicit NMD and produces a truncated protein. We examined the effects of RUNX1^{R320*} on transcription, DNA binding, and promoter-enhancer interactions using a combination of RNA-seq, ChIP-seq, and Global RNA Interactions with DNA followed by deep sequencing (GRID-seq). Our analysis revealed a RUNX1^{R320*} transcriptional signature, which is distinct from that induced by RUNX1 depletion. Interestingly, although we detected similar genome-wide binding between RUNX1 and RUNX1^{R320*}, we identified extensive remodeling of enhancer-promoter networks in RUNX1^{R320*} cells. Analysis of RUNX1^{R320*} regulated enhancer-promoter pairs detected significant enrichment of FOXK2 motifs, suggesting a novel role for FOXK2 at enhancers in conjunction with RUNX1^{R320*}. At the MYC locus we

found that RUNX1^{R320*} and FOXK2 both exhibit increased binding at hematopoietic MYC enhancers while RNA-seq detected significant MYC upregulation in RUNX1^{R320*} cells. Collectively, we demonstrate that non-RHD RUNX1 mutants can produce proteins that do not act as simple loss of function and dysregulate hematopoiesis through distinct mechanisms and cofactor interactions.

Methods

A complete description of all methods is provided in the Supplementary Methods section.

RNA-seq, ChIP-seq and GRID-seq of RUNX1 and RUNX1^{R320*} cells

RNA extraction was performed in triplicate using TRIzol (Invitrogen # 15596026) in accordance with manufacturer's protocol, library preparation and sequencing was performed by Novogene. ChIP-seq samples were prepared as described previously[15] with minor modifications using anti-RUNX1 antibody from Abcam (#23980). GRID-seq libraries from RUNX1 WT and RUNX1^{R320*} cells were prepared as previously described[16,17].

Results

RUNX1 mutations outside the RHD are not subject to NMD and can produce DNA-binding products

As a transcription factor, RUNX1 binds DNA through the runt homology domain (RHD) which lies within the N-terminal region of the protein. Pathogenic mutations detected within the RHD are frequently disrupt DNA binding and act to prevent RUNX1 function. However, the effects of mutations beyond the RHD remain poorly understood. We sought to investigate mutations beyond the RHD in more detail. To achieve this, we first assessed the distribution of hematopoietic RUNX1 mutations in the Catalogue of Somatic Mutations in Cancer (COSMIC) database[14]. We found that a significant portion of RUNX1 mutations (27%, n = 387) lie outside

the RHD and are distributed throughout the C-terminal region (Fig. 1A (top)). A high proportion of C-terminal mutations were revealed to be nonsense or frameshift (78.6%, 304 of 387) (Fig. 1B (left)). This was in stark contrast to our analysis of N-terminal/RHD regions with frameshift and nonsense accounting for only 37.3% (384 of 1030) of mutations. RUNX1 germline mutations in the RUNX1db (RUNX1 Database) also showed a similar trend of C-terminal nonsense and frameshift mutations[18]. This led us to hypothesize that this disruption of the C-terminus through frameshift or truncation was linked to the pathogenicity of these mutations and warranted further investigation.

Mutations causing frameshifts and early termination codons typically elicit nonsense mediated decay (NMD) where the premature termination codons (PTCs) lead to transcript degradation. We reasoned that the high rate of C-terminal nonsense and frameshift mutations might either elicit NMD, causing RUNX1 haploinsufficiency, or be exempt from NMD, thus producing pathogenic protein variants. The mechanisms of NMD are well defined at the transcript level and enable NMD prediction[19–22]. Briefly, only premature termination codons in the last exon and within 50 nucleotides of exon-exon junctions will not be subject to NMD. In the context of the RUNX1 transcript, PTCs beyond residue 305 of 480 (RUNX1c NM_001754.5) are predicted to be exempt from NMD (Fig. 1A (bottom)). We found that the large majority (232 of 304; 76.3%) of C-terminal frameshift and nonsense mutations were predicted to be exempt from NMD and produce proteins (Fig. 1B (right)). Together, our analysis demonstrated the most common C-terminal RUNX1 mutations are frameshift or nonsense (78.6%), and most of these mutations are projected to produce proteins with truncated or novel C-termini (76.3%), representing a class of pathogenic RUNX1 mutations distinctly different than those found within the RHD.

Pathogenic mutation RUNX1^{R320*} results in a truncated RUNX1 protein expressed at high levels

To study C-terminal RUNX1 mutations we elected to generate a homozygous

knock-in of the pathogenic RUNX1^{R320*} mutation (ClinVar: VCV000618862.12) using CRISPR-Cas9 technology in the K562 human leukemia cell line derived from a chronic myeloid leukemia patient at blast crisis (Fig. 1C, D). RUNX1^{R320*} generates a premature stop codon predicted to be exempt from NMD mechanisms, representing the majority of C-terminal RUNX1 mutations in our analysis. The RUNX1^{R320*} transcript was confirmed to produce a protein product via immunoblot (Fig. 1E). We observed a 2.37 fold increase in RUNX1^{R320*} protein relative to wild-type as well as increased transcript expression (Fig. 1F), which we hypothesize may be due to reported autoregulation of RUNX1[23]. The remaining RUNX family members, RUNX2 and RUNX3 have been reported to compensate for RUNX1 loss[24–26]. Although we detected a significant change in transcript expression of RUNX3, protein levels were barely detectable (Fig. S1A) which enabled us to study the effects RUNX1^{R320*} as the predominate RUNX protein in our model. These data demonstrate that endogenous knock-in of RUNX1^{R320*} is not subject to transcript degradation and results in the production of a truncated RUNX1 protein which is expressed at a level higher than wild-type RUNX1.

Truncation of RUNX1 blocks megakaryocyte differentiation

RUNX1 plays roles throughout hematopoiesis and has been well-described as an essential factor in megakaryocyte (MK) development as well as platelet production and function[27–29]. To investigate whether RUNX1^{R320*} dysregulates K562 cells differentiation into megakaryocytes upon induction with 12-O-tetradecanoylphorbol-13-acetate (TPA)[30], both RUNX1 and RUNX1^{R320*} cells were treated with TPA and changes in cell morphology and surface markers were assessed after 48 hours. RUNX1 wild-type cells showed characteristic megakaryocytic differentiation upon TPA treatment including the appearance of large cells with lobated nuclei, however, RUNX1^{R320*} cells produced dysplastic megakaryocyte-like cells which were smaller

with dyslobated nuclei (Fig. 2A). Undifferentiated K562 cells express CD235a, a maker presented on megakaryocytic-erythroid progenitors (MEPs) and lack the megakaryocytic lineage marker CD61. Upon TPA treatment RUNX1 wild-type cells lost CD235a and gained CD61, demonstrating megakaryocytic differentiation (Fig. 2B,C). RUNX1^{R320*} cells showed significantly less differentiation, confirming our results in Fig. 2A. Together, our data show that endogenous expression of RUNX1^{R320*} results in partial megakaryocytic differentiation block.

RUNX1^{R320*} increases DNA damage sensitivity while evading apoptosis

DNA damage as an oncogenic driver plays an important role in hematologic malignancies. RUNX1 aberrations have been shown to increase DNA damage [25,31–34]. We next sought to examine whether endogenously expressed RUNX1^{R320*} may affect these DNA damage pathways. We treated RUNX1 and RUNX1^{R320*} cells with DNA damaging agent etoposide (ETOP) and assessed DNA damage sensing through γ-H2AX imaging (Fig. S1B). RUNX1^{R320*} cells were significantly more sensitive to ETOP treatment compared to wild-type cells (Fig. 2D); similar results were observed upon camptothecin induced damage (data not shown). We hypothesized that RUNX1^{R320*} induced DNA damage sensitivity may lead to increased apoptosis. Interestingly, extended etoposide treatment over 48 hours did not result in significantly increased apoptosis in RUNX1^{R320*} cells relative to wild-type cells (Fig. S1C). Together, these results demonstrate that RUNX1^{R320*} cells become sensitized to DNA damage while evading cell death via apoptosis and suggest DNA damage sensitivity as a pathogenic attribute of RUNX1 C-terminal mutants[32].

RUNX1^{R320*} Causes Transcriptional Changes Distinct from RUNX1 Depletion

Next, we sought to investigate the impact of RUNX1^{R320*} on gene expression and disease pathways. RUNX1 influences gene expression through both direct DNA binding and protein-protein interactions with an abundance of cofactors (reviewed in [1]). As a transcriptional master regulator, mutations in RUNX1 lead to aberrant gene expression and we hypothesized that

RUNX1^{R320*} may uniquely disrupt transcription as RUNX1^{R320*} retains the DNA-binding RHD. RNA-seq followed by principal component analysis (PCA) clearly indicated RUNX1^{R320*} samples generated different transcriptome signatures than that of wild-type RUNX1 samples (Fig. 3A). Subsequent differential expression analysis revealed 1,013 upregulated genes and 1,663 downregulated genes (FDR ≤ 0.05; |log2FC| ≥ 1.5), demonstrating significant transcriptional reprogramming by RUNX1^{R320*} (Fig. 3B).

To elucidate how RUNX1^{R320*} may alter transcription differently than RUNX1 RHD loss of function mutants we compared RUNX1^{R320*} dysregulated genes to our previously generated RUNX1 knockdown RNA-seq dataset in K562 cells[35] (Fig. 3C,S2A). Remarkably, the majority (74.63%) of genes dysregulated in RUNX1^{R320*} were unique and not perturbed in RUNX1-depleted cells. Furthermore, among this small subset of commonly dysregulated genes only 62.0% of these overlapping genes were dysregulated in the same manner (both up or downregulated) between RUNX1^{R320*} and RUNX1 depleted datasets. These data demonstrate that RUNX1^{R320*} results in significant changes in transcription, dysregulating 2,676 genes and these represent a unique transcriptional signature that differs from that induced by RUNX1 depletion.

Truncation of RUNX1 dysregulates differentiation and oncogenic signaling pathways

Exploring the distinct RUNX1^{R320*} gene expression signature further, we performed overrepresentation pathway analysis on both our RUNX1^{R320*} and RUNX1 KD datasets. In line with our observed phenotypic changes, we detected significant enrichment of pathways related to megakaryocyte and platelet function (Fig. 3D). These pathways relate to the known role of RUNX1 in hematopoietic disease as well as megakaryocyte differentiation and function[27,29,36–38]. We also performed gene set enrichment analysis (GSEA)[39] and revealed negative enrichment of RUNX1 regulated megakaryocytic and hematopoietic stem cell differentiation gene sets in RUNX1^{R320*} cells (Fig. 3E). We identified specific hematopoietic genes that were dysregulated in

RUNX1^{R320*} cells using Reactome and gene ontology (GO) databases (Fig. S2B). Furthermore, several oncogenic pathways such as PI3K/AKT and MAPK signaling were uniquely enriched in our RUNX1^{R320*} dataset (Fig. 3D). GSEA also uncovered enrichment of MYC oncogenic signaling (Fig. 3F). c-MYC, a well-established leukemogenic driver[40–43], was significantly upregulated in RUNX1^{R320*} cells (Fig. 3F,G). Together, these data suggest that RUNX1^{R320*} disrupts key MK and HSC differentiation pathways while upregulating oncogenic signaling through the dysregulation of both unique genes and known RUNX1 targets.

RUNX1 and RUNX1^{R320*} exhibit similar DNA binding across the genome

We demonstrated that RUNX1^{R320*} dysregulates hematopoietic gene expression, including genes directly related to disease phenotypes (Fig. 3). As a master regulator, RUNX1 has been demonstrated to regulate gene expression through promoter and enhancer regulation as well as through chromatin remodeling[30,42,44–46]. We hypothesized that the transcriptional changes we observed in RUNX1^{R320*} cells might result from a combination of altered DNA binding and changes in cofactor interactions.

To explore changes between RUNX1 and RUNX1^{R320*} DNA binding we performed ChIP-seq. Detailed peak annotation revealed that 39.8% of RUNX1 peaks were within promoter regions, 29.8% intronic, 20.6% intergenic, 5.5% exonic, and 4.3% in 3'UTR and 5'UTR (Fig. 4A). Our findings are consistent with previously reported RUNX1 ChIP-seq datasets[30,47] (Fig. S3A-D). As the RHD is retained in RUNX1^{R320*}, we hypothesized that the loss of the C-terminus would dysregulate binding at a subset of RUNX1 sites through alterations in cofactor interactions and DNA binding may also be changed as regions of the C-terminus have been reported to have auto-inhibitory functions[6,48]. We first compared RUNX1 and RUNX1^{R320*} ChIP-seq datasets and uncovered similar binding annotation patterns: 42.7% of RUNX1^{R320*} peaks at promoter regions, 27.5% intronic, 19.3% intergenic, and 5.6% exonic with the remainder 5'/3' UTR and downstream accounting for 5.0% of peaks (Fig. 4B). Despite the increased expression of

RUNX1^{R320*} (Fig. 1E), we found that the majority of peaks (50,596) were detected in both RUNX1 and RUNX1^{R320*} datasets, demonstrating that both proteins exhibit similar genomic binding. We detected 1,061 sites of significantly downregulated RUNX1^{R320*} binding while 129 sites showed an increase in RUNX1^{R320*} presence (Fig. 4C). These data suggest that RUNX1 and RUNX1^{R320*} bind similarly throughout the genome, displaying differential binding at a small subset of sites. These data also point toward further RUNX1^{R320*} mediated gene regulation through altered interactions with co-activators/co-repressors, enhancers, and chromatin modifiers.

Loss of the C-terminus of RUNX1 alters binding at enhancers

To investigate RUNX1^{R320*} transcriptional regulation at promoters we integrated our ChIP-seq and RNA-seq datasets to examine RUNX1 and RUNX1^{R320*} bound genes (Fig. 4D). RUNX1^{R320*} promoter binding was correlated with gene expression. However, as we detected RUNX1^{R320*} binding beyond promoter regions, we hypothesized that additional regulatory elements played a role in the RUNX1^{R320*} transcriptional changes that we observed. To annotate RUNX1^{R320*} binding we divided the genome into 5 major categories: enhancers, promoters, transcribed regions, repressed regions, and heterochromatin using publicly available K562 histone modification ChIP-seq datasets (Fig. 4E)[49,50]. Both RUNX1 and RUNX1^{R320*} differentially bound sites (Fig. 4E “up/down”) and shared sites (Fig. 4E “nc”) were enriched at promoter and enhancer regions. We conducted further analysis of RUNX1 motif density at differentially bound promoters and enhancers. Enhancers with altered binding were more strongly associated with the RUNX1 DNA binding motif relative to promoter regions (Fig. 4F). These analyses demonstrate that the RUNX1 C-terminal region is required for binding at a subset of RUNX1 target sites and these dysregulated sites are strongly enriched for enhancer regions. Collectively, our data suggest a role for RUNX1^{R320*} at enhancer regions in transcription regulation in addition to canonical promoter binding.

GRID-seq identifies extensive enhancer-promoter network remodeling in RUNX1^{R320*} cells

Enhancers have been shown to play critical roles in both normal and abnormal hematopoiesis [41,51–54] and we hypothesized that RUNX1^{R320*} may dysregulate critical enhancer-promoter connections based on our RNA- and ChIP-seq analyses. To uncover these connections, we employed Global RNA Interactions with DNA by deep sequencing (GRID-seq) to map genome-wide RNA-DNA interactions and generated enhancer-promoter (E-P) network maps in RUNX1 and RUNX1^{R320*} cells[16,17]. GRID-seq detects RNA-DNA interactions using a bivalent linker to capture RNA and DNA molecules in close proximity. Nascent RNAs proximal to its endogenous promoter region as well as any associated enhancers are detected as enhancer-promoter pairs (Fig. 5A).

We separated GRID-seq interactions into “local”, “cis”, and “trans” interactions. RNA is most likely proximal to the DNA it is transcribed from, typically the gene body, these interactions we define as “local”. Beyond the gene body, “cis” interactions are between RNA and DNA regions within the same chromosome and are most likely to represent enhancer-promoter pairs while “trans” interactions are interchromosomal. As shown in Fig. 5B, local interactions are the most readily detected followed by cis interactions. Trans interactions are significantly more rare and typically weaker by orders of magnitude[55,56]. Generally, chromosomal interactions follow power law scaling enabling mathematical modeling for probability of DNA contacts, described in detail by Lieberman-Aiden et al. and others[52,57]. Our GRID-seq datasets successfully recapitulated these findings (Fig. 5C) and allowed us to apply this model to GRID-seq detected local, cis, and trans interactions, ranking them and generating a Z-score scale in RUNX1 and RUNX1^{R320*} cells. Examining cis interactions between RUNX1 and RUNX1^{R320*} datasets, we detected 30,365 interactions unique to RUNX1 and 32,903 RUNX1^{R320*} specific interactions with 52,089 occurring in both (Fig. 5D). E-P pairs that were up and down regulated in RUNX1^{R320*} cells were correlated with respective increases and decreases in gene expression (Fig. S3E). Furthermore,

our data revealed extensive interaction remodeling at differentially expressed hematopoietic and platelet gene loci such as KIT, DIAPH1, NFE2, and STIM1 (Fig. S4A-D). Together our GRID-seq dataset in combination with ChIP-seq and gene expression analysis establishes that RUNX1^{R320*} broadly alters enhancer-promoter networks leading to significant transcriptional dysregulation.

RUNX1^{R320*} and FOXK2 enrichment at enhancers and MYC regulation

We hypothesized that RUNX1^{R320*} may remodel enhancer-promoter networks through cofactor interactions either gained or lost upon the truncation of the RUNX1 C-terminus. RUNX1^{R320*} specific enhancer-promoter pairs were examined for cofactor motifs. Using this approach, we successfully detected enrichment of the RUNX motif in addition to ETS1/PU.1, factors known to cooperate with RUNX1 at enhancers and promoters. We also identified forkhead box (FOX) family motifs as significantly enriched at RUNX1^{R320*} regulated E-P pairs, including those shared with RUNX1 (Fig. 5E). FOX proteins are a large family of DNA binding factors which play a variety of roles throughout different lineages, including enhancer regulation[58–60]. We next asked which FOX proteins were expressed in our leukemia model. We determined that the FOXK subfamily had the significantly higher expression in both RUNX1 wild-type and RUNX1^{R320*} cells (Fig. 5F). FOXK2 but not FOXK1 showed co-occupancy at RUNX1 sites in ENCODE datasets (Fig. S5A). Furthermore, FOXK2 and RUNX1 protein interaction network analysis also revealed shared overlapping proteins (Fig. S5B). Together, our analyses suggest a role for FOXK2 at RUNX1^{R320*} regulated enhancer-promoter networks.

To further explore the potential role of FOKX2 at RUNX1^{R320*} bound enhancers we examined the well-described RUNX1-bound MYC super enhancer locus, where we detected significant E-P remodeling in GRID-seq (Fig. 6A) and upregulation of MYC and MYC signaling (Fig. 3F,G). RUNX1 has been reported to bind element 3 (E3) of the BENC (Blood ENhancer Cluster) super

enhancer[42,43,61,62]. We theorized that RUNX1^{R320*} may dysregulate or hijack this super enhancer to affect MYC expression in conjunction with FOXK2 in the context of our model.

To build upon RUNX1 WT ENCODE H3K27ac and FOXK2 data and assess the presence of these factors in RUNX1^{R320*} cells at MYC enhancer loci we performed Cleavage Under Targets & Release Using Nuclease (CUT&RUN)[63] followed by qPCR in RUNX1 and RUNX1^{R320*} cells. We confirmed RUNX1 binding at E3 and detected significantly higher RUNX1^{R320*} binding at this enhancer (Fig. 6B). FOXK2 binding at E3 was also significantly increased in RUNX1^{R320*} cells (Fig. 6C). The SWI/SNF component BRG1 has been suggested to play an activating role at MYC enhancer regions[61], however, we detected no significant change in BRG1 binding at E3 between RUNX1 WT and RUNX1^{R320*} cells (Fig. S6A). We also observed increased RUNX1^{R320*} and FOXK2 binding at the NOTCH-bound MYC enhancer (N-Me) (Fig. S6B, C). However, H3K27ac signal was not present in this region indicating the potential requirement for additional cofactors for N-Me activation.

To further investigate the effect of FOXK2 on MYC expression we performed shRNA mediated FOXK2 knockdown (Fig. 6D). The level of c-MYC was significantly reduced in both WT and RUNX1^{R320*} cells upon FOXK2 knockdown relative to a non-targeting shRNA control (Fig. 6E and Fig. S6D, E). Together, these data suggest a potential role for FOXK2 in RUNX1^{R320*} mediated enhancer-promoter networks as well as the upregulation of MYC and MYC oncogenic signaling via the BENC super-enhancer (Fig. 6F).

Discussion

In this work we study how RUNX1 mutations outside the runt homology domain promote abnormal hematopoiesis. We reveal that mutations in the C-terminus of RUNX1 are mainly nonsense or frameshift and remain largely exempt from NMD, producing mutated proteins capable of DNA binding. We note that frameshift mutations may result in novel C-termini but focus on the effects of the retained portion of RUNX1 in this study. Modeling this class of

mutation through endogenous gene editing and expression of RUNX1^{R320*}, we detected a unique gene expression signature that differs from that induced by RUNX1 depletion. This suggests that the truncation of the RUNX1 C-terminus does not function simply as a loss of function mutation. We demonstrate that this aberrant transcriptional program contributes to disease phenotypes including megakaryocytic differentiation block and disruption of hematopoietic and oncogenic pathways. Upon further investigation, we uncovered remodeling of enhancer-promoter networks in RUNX1^{R320*} cells using GRID-seq. Analysis of altered E-P pairs revealed significant enrichment of the FOX transcription factor motif that led us to examine FOXK2. Our results suggest a novel potential role for FOXK2 and RUNX1^{R320*}in the alteration of enhancer-promoter networks leading to dysregulated hematopoiesis.

Our work investigates the RUNX1 C-terminus which has been shown to harbor pathogenic mutations across hematologic malignancies, yet these mechanisms remain incompletely understood. These mutations retain the DNA-binding RHD and therefore exhibit binding to RUNX motifs. Previous in vitro studies suggest that the C-terminus of RUNX1 contains multiple intramolecular inhibitory regions that impair DNA binding[6,48,67]. Interestingly, our ChIP-seq data show that RUNX1 and RUNX1^{R320*} bind to DNA similarly. We hypothesize that our study reflects an endogenous context where cofactor complexes act to closely regulate RUNX1 DNA binding. Furthermore, RUNX1 frequently interacts with other hematopoietic transcription factors to co-regulate critical genes (reviewed in[68]). Additionally, RUNX1 interacts with DNA in the context of chromatin looping and interacts with both cohesin complex subunit STAG2[44] and multiple chromatin remodelers such PRC1[61,69] and SWI/SNF[43] complexes. Our data suggests that in an endogenous environment RUNX1 DNA binding is modulated through interactions with a combination of factors, which culminates in similar RUNX1 and RUNX1^{R320*} binding on a genome-wide scale. Further studies are required to unravel the combinatorial influences behind RUNX1^{R320*} DNA binding at target sites.

Additionally, the loss of the multi-functional carboxy-terminus of RUNX1 removes two highly conserved RUNX family domains, the nuclear matrix targeting signal (NMTS) and the terminal VWRPY domain. Independent of DNA-binding, the NMTS has been reported to be critical for subnuclear localization and cooperation with PU.1, a critical hematopoietic transcription factor[70,71]. We hypothesize that mislocalization of RUNX1^{R320*} alters its subnuclear availability and interactions with nuclear matrix factors resulting in unique transcriptional perturbations. Furthermore, the conserved VWRPY domain, essential for megakaryopoiesis and HSC maturation[72], binds the TLE1 corepressor and represses RUNX1 activity[7,73]. Lacking TLE1 binding may allow RUNX1^{R320*} to act as an activator at a subset of sites typically repressed by full-length RUNX1, a hypothesis supported by our transcriptome analysis. Taken together, we reason that the truncation of RUNX1 alters its subnuclear localization and ability to interact with various cofactors, resulting in unconventional RUNX1^{R320*} complexes and transcriptional dysregulation of hematopoietic pathways.

Upon the truncation of RUNX1 enhancer-promoter networks are significantly distorted. At dysregulated E-P pairs we found significant enrichment of the forkhead box (FOX) DNA binding motif shared among FOX family members. A large family of 44 conserved transcription factors, FOX proteins act to regulate transcription through both direct DNA binding and cooperation with lineage specific factors. Of the 14 subfamilies, the FOXK family, which consists of FOXK1 and FOXK2, was most highly expressed in our leukemia model. Although FOXK2 is understudied in the hematopoietic system and unlike FOXK1, ENCODE datasets suggest RUNX1 and FOXK2 DNA binding sites frequently overlap. Previous studies depict a bivalent role for FOXK2, activating and repressing transcription in a context dependent manner[74–76]. Our data suggest that the loss of the C-terminus of RUNX1 may allow further cooperation between FOXK2 and RUNX1^{R320*} which act to regulate a subset of enhancer-promoter connections such as the BENC MYC super-enhancer.

In summary, we establish that RUNX1 C-terminal variants consist mostly of nonsense and frameshift mutations which are largely exempt from nonsense mediated decay and lead to the production of truncated RUNX1 proteins. These proteins dysregulate hematopoietic transcriptional programs in a manner that is distinct from RUNX1 depletion. Upon further investigation we show that the loss of the domains in the C-terminus of RUNX1 results in the remodeling of enhancer-promoter networks where we uncover a potential role for FOXK2 in cooperation with RUNX1^{R320*} in enhancer regulation.

Contribution: N.D.J. and D.-E.Z. devised the study and designed the experimental strategies; N.D.J. performed the research, collected the data, and analyzed the results; D.-H.L. and P.B.C. prepared the GRID-seq and ChIP-seq libraries respectively; Z.L. performed bioinformatic analyses pertaining to GRID-seq datasets; C.D. and L.X. performed microscopy-based data collection and analysis. K.-I.A. assisted in protein expression/interaction experiments. M.L. assisted in flow cytometry experiments and related statistical analysis. N.D.J. wrote the manuscript; X.-D.F., and B.R. provided resources, imparted expertise, and critically reviewed the manuscript; and D.-E.Z. oversaw the study, supervised manuscript preparation, and secured funding to support the study.

COI: B.R. is a cofounder of Epigenome Technologies, Inc. and has equity in Arima Genomics, Inc. The remaining authors declare no conflict of interest.

References

1. Sood R, Kamikubo Y, Liu P. Role of RUNX1 in hematological malignancies. *Blood*. 2017;129(15):2070-2082. doi:10.1182/blood-2016-10-687830

2. Chen MJ, Yokomizo T, Zeigler BM, Dzierzak E, Speck NA. Runx1 is required for the endothelial to haematopoietic cell transition but not thereafter. *Nature*. 2009;457(7231):887-891. doi:10.1038/nature07619

3. Wang Q, Stacy T, Binder M, Marín-Padilla M, Sharpe AH, Speck NA. Disruption of the Cbfa2 gene causes necrosis and hemorrhaging in the central nervous system and blocks definitive hematopoiesis. *Proc Natl Acad Sci U S A*. 1996;93(8):3444-3449. doi:10.1073/pnas.93.8.3444

4. Okuda T, Van Deursen J, Hiebert SW, Grosveld G, Downing JR. AML1, the target of multiple chromosomal translocations in human leukemia, is essential for normal fetal liver hematopoiesis. *Cell*. 1996;84(2):321-330. doi:10.1016/S0092-8674(00)80986-1

5. Dowdy CR, Xie R, Frederick D, et al. Definitive hematopoiesis requires Runx1 C-terminal-mediated subnuclear targeting and transactivation. *Hum Mol Genet*. 2010;19(6):1048-1057. doi:10.1093/hmg/ddp568

6. Gu TL, Goetz TL, Graves BJ, Speck NA. Auto-inhibition and partner proteins, core-binding factor beta (CBFbeta) and Ets-1, modulate DNA binding by CBFalpha2 (AML1). *Mol Cell Biol*. 2000;20(1):91-103. http://www.ncbi.nlm.nih.gov/pubmed/10594012%0Ahttp://www.pubmedcentral.nih.gov/articlerender.fcgi?artid=PMC85059.

7. Imai Y, Kurokawa M, Tanaka K, et al. TLE, the human homolog of Groucho, interacts with AML1 and acts as a repressor of AML1-induced transactivation. *Biochem Biophys Res Commun*. 1998;252(3):582-589. doi:10.1006/bbrc.1998.9705

8. Osato M, Asou N, Abdalla E, et al. Biallelic and heterozygous point mutations in the runt domain of the AML1/PEBP2αB gene associated with myeloblastic leukemias. *Blood*. 1999;93(6):1817-1824. doi:10.1182/blood.v93.6.1817.406k36_1817_1824

9. Harada H, Harada Y, Niimi H, Kyo T, Kimura A, Inaba T. High incidence of somatic mutations in the AML1/RUNX1 gene in myelodysplastic syndrome and low blast percentage myeloid leukemia with myelodysplasia. *Blood*. 2004;103(6):2316-2324. doi:10.1182/blood-2003-09-3074

10. Kuo MC, Liang DC, Huang CF, et al. RUNX1 mutations are frequent in chronic myelomonocytic leukemia and mutations at the C-terminal region might predict acute myeloid leukemia transformation. *Leukemia*. 2009;23(8):1426-1431. doi:10.1038/leu.2009.48

11. Owen CJ, Toze CL, Koochin A, et al. Five new pedigrees with inherited RUNX1 mutations causing familial platelet disorder with propensity to myeloid malignancy. *Blood*. 2008;112(12):4639-4645. doi:10.1182/blood-2008-05-156745

12. Song WJ, Sullivan MG, Legare RD, et al. Haploinsufficiency of CBFA2 causes familial thrombocytopenia with propensity to develop acute myelogenous leukaemia. *Nat Genet*. 1999;23(2):166-175. doi:10.1038/13793

13. Homan C, Scott H, Brown A. Hereditary platelet disorders associated with germline

variants in RUNX1, ETV6 and ANKRD26. 2022.

14. Tate JG, Bamford S, Jubb HC, et al. COSMIC: The Catalogue Of Somatic Mutations In Cancer. *Nucleic Acids Res*. 2019;47(D1):D941-D947. doi:10.1093/nar/gky1015

15. Huang H, Zhu Q, Jussila A, et al. CTCF mediates dosage- and sequence-context-dependent transcriptional insulation by forming local chromatin domains. *Nat Genet*. 2021;53(7):1064-1074. doi:10.1038/s41588-021-00863-6

16. Li X, Zhou B, Chen L, Gou LT, Li H, Fu XD. GRID-seq reveals the global RNA-chromatin interactome. *Nat Biotechnol*. 2017;35(10):940-950. doi:10.1038/nbt.3968

17. Zhou B, Li X, Luo D, Lim DH, Zhou Y, Fu XD. *GRID-Seq for Comprehensive Analysis of Global RNA–Chromatin Interactions*. Vol 14. Springer US; 2019. doi:10.1038/s41596-019-0172-4

18. Homan CC, King-Smith SL, Lawrence DM, et al. The RUNX1 Database (RUNX1db): establishment of an expert curated RUNX1 registry and genomics database as a public resource for familial platelet disorder with myeloid malignancy. *Haematologica*. 2021;106(11):3004-3007. doi:10.3324/haematol.2021.278762

19. Lykke-Andersen S, Jensen TH. Nonsense-mediated mRNA decay: An intricate machinery that shapes transcriptomes. *Nat Rev Mol Cell Biol*. 2015;16(11):665-677. doi:10.1038/nrm4063

20. Popp MW, Maquat LE. Nonsense-mediated mRNA Decay and Cancer. *Curr Opin Genet Dev*. 2018;48:44-50. doi:10.1016/j.gde.2017.10.007

21. Hu Z, Yau C, Ahmed AA. A pan-cancer genome-wide analysis reveals tumour dependencies by induction of nonsense-mediated decay. *Nat Commun*. 2017;8(May):1-9. doi:10.1038/ncomms15943

22. Supek F, Lehner B, Lindeboom RGH. To NMD or Not To NMD: Nonsense-Mediated mRNA Decay in Cancer and Other Genetic Diseases. *Trends Genet*. 2021;37(7):657-668. doi:10.1016/j.tig.2020.11.002

23. Martinez M, Hinojosa M, Trombly D, et al. Transcriptional auto-regulation of RUNX1 P1 promoter. *PLoS One*. 2016;11(2):1-17. doi:10.1371/journal.pone.0149119

24. Kamikubo Y. Genetic compensation of RUNX family transcription factors in leukemia. *Cancer Sci*. 2018;109(8):2358-2363. doi:10.1111/cas.13664

25. Wang CQ, Krishnan V, Tay LS, et al. Disruption of Runx1 and Runx3 Leads to Bone Marrow Failure and Leukemia Predisposition due to Transcriptional and DNA Repair Defects. *Cell Rep*. 2014;8(3):767-782. doi:10.1016/J.CELREP.2014.06.046

26. Goyama S, Schibler J, Cunningham L, et al. Transcription factor RUNX1 promotes survival of acute myeloid leukemia cells. *J Clin Invest*. 2013;123(9):3876-3888. doi:10.1172/JCI68557DS1

27. Lee K, Ahn HS, Estevez B, Poncz M. RUNX1-deficient human megakaryocytes demonstrate thrombopoietic , and platelet half-life and functional defects. *Blood*. 2022. doi:10.1182/blood.2022017561

28. Ichikawa M, Yoshimi A, Nakagawa M, Nishimoto N, Watanabe-Okochi N, Kurokawa M. A role for RUNX1 in hematopoiesis and myeloid leukemia. *Int J Hematol*. 2013;97(6):726-

734. doi:10.1007/s12185-013-1347-3

29. Estevez B, Borst S, Jarocha D, et al. RUNX-1 haploinsufficiency causes a marked deficiency of megakaryocyte-biased hematopoietic progenitor cells. *Blood*. 2021;137(19):2662-2675. doi:10.1182/blood.2020006389

30. Pencovich N, Jaschek R, Tanay A, Groner Y, Dc W. Dynamic combinatorial interactions of RUNX1 and cooperating partners regulates megakaryocytic differentiation in cell line models. *Blood*. 2012;117(1):1-15. doi:10.1182/blood-2010-07-295113

31. Wu D, Ozakis T, Yoshiharas Y, et al. Runt-related Transcription Factor 1 (RUNX1) Stimulates Tumor Suppressor p53 Protein in Response to DNA Damage through Complex Formation and Acetylation. *J Biol Chem*. 2013;288(2):1353-1364. doi:10.1074/jbc.M112.402594

32. Satoh Y, Matsumura I, Tanaka H, et al. C-terminal mutation of RUNX1 attenuates the DNA-damage repair response in hematopoietic stem cells. *Leukemia*. 2012;26(2):303-311. doi:10.1038/leu.2011.202

33. Samarakkody AS, Shin NY, Cantor AB. Role of RUNX Family Transcription Factors in DNA Damage Response. *Mol Cells*. 2020;43(2):99-106. doi:10.14348/molcells.2019.0304

34. Tay LS, Krishnan V, Sankar H, et al. RUNX Poly(ADP-Ribosyl)ation and BLM Interaction Facilitate the Fanconi Anemia Pathway of DNA Repair. *Cell Rep*. 2018;24(7):1747-1755. doi:10.1016/j.celrep.2018.07.038

35. Huang Y-J, Chen J-Y, Yan M, et al. RUNX1 deficiency cooperates with SRSF2 mutation to induce multilineage hematopoietic defects characteristic of MDS. *Blood Adv*. 2022;6(23):6078-6092. doi:10.1182/bloodadvances.2022007804

36. Ichikawa M, Asai T, Saito T, et al. AML-1 is required for megakaryocytic maturation and lymphocytic differentiation, but not for maintenance of hematopoietic stem cells in adult hematopoiesis. *Nat Med*. 2004;10(3):299-304. doi:10.1038/nm997

37. Wang C, Tu Z, Cai X, et al. A Critical Role of RUNX1 in Governing Megakaryocyte-Primed Hematopoietic Stem Cell Differentiation. *Blood Adv*. 2023;7(11):2590-2605. doi:10.1182/bloodadvances.2022008591

38. Sakurai M, Kunimoto H, Watanabe N, et al. Impaired hematopoietic differentiation of RUNX1-mutated induced pluripotent stem cells derived from FPD/AML patients. *Leukemia*. 2014;28(12):2344-2354. doi:10.1038/leu.2014.136

39. Subramanian A, Tamayo P, Mootha VK, et al. Gene set enrichment analysis: A knowledge-based approach for interpreting genome-wide expression profiles. *Proc Natl Acad Sci*. 2005;102(43):15545-15550. doi:10.1073/pnas.0506580102

40. Wotton S, Stewart M, Blyth K, et al. Proviral insertion indicates a dominant oncogenic role for Runx1/AML-1 in T-cell lymphoma. *Cancer Res*. 2002;62(24):7181-7185.

41. Simeoni F, Romero-Camarero I, Camera F, et al. Enhancer recruitment of transcription repressors RUNX1 and TLE3 by mis-expressed FOXC1 blocks differentiation in acute myeloid leukemia. *Cell Rep*. 2021;36(12):109725. doi:10.1016/j.celrep.2021.109725

42. Choi Ah, Illendula A, Pulikkan JA, et al. RUNX1 is required for oncogenic Myb and Myc enhancer activity in T-cell acute lymphoblastic leukemia. *Blood*. 2017;130(15):1722-1733. doi:10.1182/blood-2017-03-775536

43. Shi J, Whyte WA, Zepeda-Mendoza CJ, et al. Role of SWI/SNF in acute leukemia maintenance and enhancer-mediated Myc regulation. *Genes Dev*. 2013;27(24):2648-2662. doi:10.1101/gad.232710.113

44. Ochi Y, Kon A, Sakata T, et al. Combined Cohesin–RUNX1 deficiency synergistically perturbs chromatin looping and causes myelodysplastic syndromes. *Cancer Discov*. 2020;10(6):836-853. doi:10.1158/2159-8290.CD-19-0982

45. Barutcu AR, Hong D, Lajoie BR, et al. RUNX1 contributes to higher-order chromatin organization and gene regulation in breast cancer cells. *Biochim Biophys Acta - Gene Regul Mech*. 2016;1859(11):1389-1397. doi:10.1016/j.bbagrm.2016.08.003

46. Bowers SR, Calero-Nieto FJ, Valeaux S, Fernandez-Fuentes N, Cockerill PN. Runx1 binds as a dimeric complex to overlapping Runx1 sites within a palindromic element in the human GM-CSF enhancer. *Nucleic Acids Res*. 2010;38(18):6124-6134. doi:10.1093/nar/gkq356

47. Beck D, Thoms JAI, Perera D, et al. Genome-wide analysis of transcriptional regulators in human HSPCs reveals a densely interconnected network of coding and noncoding genes. *Blood*. 2013;122(14):e12-e22. doi:10.1182/blood-2013-03-490425

48. Kanno T, Kanno Y, Chen L-F, Ogawa E, Kim W-Y, Ito Y. Intrinsic Transcriptional Activation-Inhibition Domains of the Polyomavirus Enhancer Binding Protein 2/Core Binding Factor α Subunit Revealed in the Presence of the β Subunit. *Mol Cell Biol*. 1998;18(5):2444-2454. doi:10.1128/mcb.18.5.2444

49. Dunham I, Kundaje A, Aldred SF, et al. An integrated encyclopedia of DNA elements in the human genome. *Nature*. 2012;489(7414):57-74. doi:10.1038/nature11247

50. Luo Y, Hitz BC, Gabdank I, et al. New developments on the Encyclopedia of DNA Elements (ENCODE) data portal. *Nucleic Acids Res*. 2020;48(D1):D882-D889. doi:10.1093/nar/gkz1062

51. Adhikary S, Roy S, Chacon J, Gadad SS, Das C. Implications of enhancer transcription and eRNAs in cancer. *Cancer Res*. 2021:canres.4010.2020. doi:10.1158/0008-5472.can-20-4010

52. Ron G, Globerson Y, Moran D, Kaplan T. Promoter-enhancer interactions identified from Hi-C data using probabilistic models and hierarchical topological domains. *Nat Commun*. 2017;8(1). doi:10.1038/s41467-017-02386-3

53. Li W, Notani D, Ma Q, et al. Functional roles of enhancer RNAs for oestrogen-dependent transcriptional activation. *Nature*. 2013;498(7455):516-520. doi:10.1038/nature12210

54. Li K, Zhang Y, Liu X, et al. Noncoding variants connect enhancer dysregulation with nuclear receptor signaling in hematopoietic malignancies. *Cancer Discov*. 2020;10(5):724-745. doi:10.1158/2159-8290.CD-19-1128

55. Schoenfelder S, Fraser P. Long-range enhancer–promoter contacts in gene expression control. *Nat Rev Genet*. 2019;20(8):437-455. doi:10.1038/s41576-019-0128-0

56. Lin D, Bonora G, Yardımcı GG, Noble WS. Computational methods for analyzing and modeling genome structure and organization. *Wiley Interdiscip Rev Syst Biol Med*. 2019;11(1):1-14. doi:10.1002/wsbm.1435

57. Lieberman-aiden E, Berkum NL Van, Williams L, et al. Comprehensive Mapping of Long-

Range Interactions Reveals Folding Principles of the Human Genome. 2009;33292(October):289-294.

58. Wang D, Garcia-Bassets I, Benner C, et al. Reprogramming transcription by distinct classes of enhancers functionally defined by eRNA. *Nature*. 2011;474(7351):390-397. doi:10.1038/nature10006

59. Xu J, Watts JA, Pope SD, et al. Transcriptional competence and the active marking of tissue-specific enhancers by defined transcription factors in embryonic and induced pluripotent stem cells. *Genes Dev*. 2009;23(24):2824-2838. doi:10.1101/gad.1861209

60. Golson ML, Kaestner KH. Fox transcription factors: From development to disease. *Dev*. 2016;143(24):4558-4570. doi:10.1242/dev.112672

61. Pulikkan JA, Hegde M, Ahmad HM, et al. CBFβ-SMMHC Inhibition Triggers Apoptosis by Disrupting MYC Chromatin Dynamics in Acute Myeloid Leukemia. *Cell*. 2018;174(1):172-186.e21. doi:10.1016/j.cell.2018.05.048

62. Herranz D, Ambesi-Impiombato A, Palomero T, et al. A NOTCH1-driven MYC enhancer promotes T cell development, transformation and acute lymphoblastic leukemia. *Nat Med*. 2014;20(10):1130-1137. doi:10.1038/nm.3665

63. Skene PJ, Henikoff S. An efficient targeted nuclease strategy for high-resolution mapping of DNA binding sites. *Elife*. 2017;6:1-35. doi:10.7554/eLife.21856

64. Farley EK, Olson KM, Zhang W, Rokhsar DS, Levine MS. Syntax compensates for poor binding sites to encode tissue specificity of developmental enhancers. *Proc Natl Acad Sci U S A*. 2016;113(23):6508-6513. doi:10.1073/pnas.1605085113

65. Yashiro-Ohtani Y, Wang H, Zang C, et al. Long-range enhancer activity determines Myc sensitivity to Notch inhibitors in T cell leukemia. *Proc Natl Acad Sci U S A*. 2014;111(46):E4946-E4953. doi:10.1073/pnas.1407079111

66. Islam R, Jenkins CE, Cao Q, et al. RUNX1 colludes with NOTCH1 to reprogram chromatin in T cell acute lymphoblastic leukemia. *iScience*. 2023;26(6). doi:10.1016/j.isci.2023.106795

67. Kim WY, Sieweke M, Ogawa E, et al. Mutual activation of Ets-1 and AML1 DNA binding by direct interaction of their autoinhibitory domains. *EMBO J*. 1999;18(6):1609-1620. doi:10.1093/emboj/18.6.1609

68. Dzierzak E, Bigas A. Blood Development: Hematopoietic Stem Cell Dependence and Independence. *Cell Stem Cell*. 2018;22(5):639-651. doi:10.1016/j.stem.2018.04.015

69. Yu M, Mazor T, Huang H, et al. Direct Recruitment of Polycomb Repressive Complex 1 to Chromatin by Core Binding Transcription Factors. *Mol Cell*. 2012;45(3):330-343. doi:10.1016/j.molcel.2011.11.032

70. Zeng C, Van Wijnen AJ, Stein JL, et al. Identification of a nuclear matrix targeting signal in the leukemia and bone-related AML/CBF-α transcription factors. *Proc Natl Acad Sci U S A*. 1997;94(13):6746-6751. doi:10.1073/pnas.94.13.6746

71. Li X, Vradii D, Gutierrez S, et al. Subnuclear targeting of Runx1 is required for synergistic activation of the myeloid specific M-CSF receptor promoter by PU.1. *J Cell Biochem*. 2005;96(4):795-809. doi:10.1002/jcb.20548

72. Alkadi H, McKellar D, Zhen T, et al. The VWRPY Domain Is Essential for RUNX1 Function in Hematopoietic Progenitor Cell Maturation and Megakaryocyte Differentiation. *Blood*. 2018;132(Supplement 1):1319. doi:10.1182/blood-2018-99-113400

73. Levanon D, Goldstein RE, Bernstein Y, et al. Transcriptional repression by AML1 and LEF-1 is mediated by the TLE/Groucho corepressors. *Proc Natl Acad Sci U S A*. 1998;95(20):11590-11595. doi:10.1073/pnas.95.20.11590

74. Shan L, Zhou X, Liu X, et al. FOXK2 Elicits Massive Transcription Repression and Suppresses the Hypoxic Response and Breast Cancer Carcinogenesis. *Cancer Cell*. 2016;30(5):708-722. doi:10.1016/j.ccell.2016.09.010

75. De Moraes N, Carneiro LD, Maia RC, Lam EWF, Sharrocks AD. Foxk2 transcription factor and its emerging roles in cancer. *Cancers (Basel)*. 2019;11(3):1-20. doi:10.3390/cancers11030393

76. Ji Z, Donaldson IJ, Liu J, Hayes A, Zeef LAH, Sharrocks AD. The Forkhead Transcription Factor FOXK2 Promotes AP-1-Mediated Transcriptional Regulation. *Mol Cell Biol*. 2012;32(2):385-398. doi:10.1128/mcb.05504-11

Acknowledgments

The authors thank the staff at the Moores Cancer Center Flow Cytometry Core Facility for generous help with fluorescence activated cell sorting and the staff at the University of California, San Diego Institute for Genomic Medicine for assistance with next-generation sequencing.

This work was supported by National Institutes of Health (NIH), National Heart, Lung, and Blood Institute grant 5F31HL152652 (N.D.J.) and NIH, National Institute of Diabetes and Digestive and Kidney Diseases grant R01DK098808 (D.-E.Z.). This work was also supported by a National Institutes of Health training grant T32GM007240 (N.D.J.) This publication includes data generated at the UC San Diego IGM Genomics Center utilizing an Illumina NovaSeq 6000 that was purchased with funding from a National Institutes of Health SIG grant (#S10 OD026929). Visual abstract and model created with BioRender.com. The University of California, San Diego Moores Cancer Center Core facilities are supported by NIH Cancer Center Support Grant (CCSG P30CA23100).

Authorship

Contribution: N.D.J. and D.-E.Z. devised the study and designed the experimental strategies; N.D.J. performed the research, collected the data, and analyzed the results; D.-H.L. and P.B.C. prepared the GRID-seq and ChIP-seq libraries respectively; Z.L. performed bioinformatic analyses pertaining to GRID-seq datasets; C.D. and L.X. performed microscopy-based data collection and analysis. K.-I.A. assisted in protein expression/interaction experiments. M.L. assisted in flow cytometry experiments and related statistical analysis. N.D.J. wrote the manuscript; X.-D.F., and B.R. provided resources, imparted expertise, and critically reviewed the manuscript; and D.-E.Z. oversaw the study, supervised manuscript preparation, and secured funding to support the study.

Conflict-of-interest disclosure: B.R. is a cofounder of Epigenome Technologies, Inc. and has equity in Arima Genomics, Inc.

655 Correspondence: Dong-Er Zhang, University of California, San Diego, 9500 Gilman Dr, Mail
656 Stop 0815, La Jolla, CA 92037; e-mail: d7zhang@health.ucsd.edu

Figure 1: C-terminal RUNX1 mutations are frequently frameshift and nonsense resulting in transcripts which are exempt from nonsense mediated decay.

(A) Lollipop plot of hematopoietic mutations in RUNX1 (isoform 1c NP_001754.2) in the COSMIC database with accompanying transcript exons displayed (top). Truncating mutations include nonsense, nonstop, frameshift deletion, frameshift insertion, splice site. In-frame deletions and in-frame insertions are considered in-frame mutations, and all other non-missense mutations are labeled as "Other." Enlarged region of exon 7 and 8 of RUNX1 denoting NMD exempt mutations (bottom). Mutations which result in a premature stop codon in the final exon (exon 8) or within 50 nucleotides upstream of the last exon-exon junction (exon 7-8) are predicted to be exempt from nonsense mediated decay (NMD). **(B)** Analysis of C-terminal RUNX1 mutations beyond the Runt homology domain (RHD). Frameshift and nonsense mutations represented 304 of 387 mutations (78.55%) while all other in frame mutations consisting of missense, in frame insertions and deletions, coding silent substitutions, and compound substitution combined account for 83 of 387 mutations (21.45%). NMD analysis was performed on the 304 frameshift and nonsense mutations, examining premature stop codons within the region defined in Fig. 1A. A total of 76.3% (232 of 304) C-terminal frameshift and nonsense mutations were predicted to exempt from NMD. **(C)** Schematic of RUNX1 protein domains and knock-in R320* mutation using CRISPR-Cas9. **(D)** Sanger sequencing of RUNX1^{R320*} homozygous knock-in mutation compared to wild-type RUNX1 sequence. K562 cells were nucleofected with Cas9, RUNX1 targeting gRNA, and R320* donor template. The gRNA (black underline) targeted exon 7 (isoform 1c NM_001754.5) and donor oligo template results in TAA codon from TCG at R320. Single cell clones were screened for homozygous mutations, confirmed by sequencing of the targeted region, and analyzed by ICE tool by Synthego. **(E)** Western blot of wild-type (WT) RUNX1 and RUNX1^{R320*} K562 cells along with β-actin loading control. Both lines were subjected to the same nucleofection process +/- CRISPR-Cas9 editing components. Whole cell lysate was extracted and used to confirm the presence of both wild-type and RUNX1^{R320*} proteins, densitometry calculations were performed using β-actin normalization. The arrow indicates a possible non-specific signal. **(F)** RUNX1 transcript levels in RUNX1 wild-type and RUNX1^{R320*} cells and RUNX family members as measured by DESeq2 analysis software package. Each line subjected to RNA-seq and sampled in triplicate (n = 3), Students t-test was used, significance: * $p \leq 0.05$; ** $p \leq 0.01$; *** $p \leq 0.001$; **** $p \leq 0.0001$.

Figure 2: RUNX1R320* results in differentiation block and increased DNA damage sensitivity.

(A) Representative images of RUNX1 wild-type and RUNX1^{R320*} cells treated with DMSO or 10 nM TPA for 48 hours. Differentiating cells are denoted with arrows. **(B-C)** Representative flow cytometry analysis of RUNX1 wild-type and RUNX1^{R320*} K562 cells which were treated with DMSO, 5 nM TPA for 48 hours. Megakaryocyte marker CD61 (integrin β3 chain) was analyzed along with the erythroid marker CD235a (glycophorin A). Live cells were divided into four groups using FACS diva software based on the presence (+/-) of CD61 and CD235a. DMSO treated control cells were compared to TPA treated cells in both RUNX1 wild-type and RUNX1^{R320*} genotypes (n = 3). Significance was determined using two-way ANOVA. **(D)** DNA damage levels in RUNX1 wild-type and RUNX1^{R320*} cells upon treatment with etoposide (ETOP) and camptothecin (CPT) relative to DMSO control. Cells were treated with 25 μM ETOP or CPT for 1 hour at 37°C before fixation and staining. DAPI was used to identify the nuclei of cells and γH2AX mean signal intensity was measured per cell within the nucleus. Student's t-test was used to determine significance. * $p \leq 0.05$; ** $p \leq 0.01$; *** $p \leq 0.001$; **** $p \leq 0.0001$.

Figure 3: RUNX1R320* results in significant transcriptional dysregulation of megakaryocytic differentiation pathways and MYC targets.

(A) Principal component analysis of RUNX1 wild-type (n = 3) and RUNX1^{R320*} (n = 3) RNA-seq samples following analysis using DESeq2. **(B)** Volcano plot showing differentially expressed genes between RUNX1 wild-type and RUNX1^{R320*} cells. Genes were considered significantly differentially expressed (red) with FDR ≤ 0.05 and fold-change ≥ ±1.5). **(C)** Comparison of differentially expressed genes between RUNX1^{R320*} and RUNX1 knockdown experiments. RUNX1^{R320*} cells were compared to RUNX1 wild-type controls and RUNX1 shRNA knockdown cells to shRNA control cells in triplicate. Both datasets were analyzed with DESeq2 with significance determined by FDR ≤ 0.05 and fold-change ≥ ±1.5. **(D)** Reactome pathway analysis of genes differentially expressed genes in RUNX1^{R320*} and RUNX1 knockdown cells described in (A-C). Pathways were considered significant with p-value < 0.05. **(E-F)** GSEA enrichment results between wild-type and RUNX1^{R320*} RNA-seq datasets, NES = normalized enrichment score. **(G)** MYC expression in RUNX1 and RUNX1^{R320*} cells via RNA-seq. Student's t-test was used to determine significance: * p ≤ 0.05; ** p ≤ 0.01; *** p ≤ 0.001; **** p ≤ 0.0001.

Figure 4: RUNX1R320* differential binding is most enriched at enhancer regions.

(A-B) Annotation of RUNX1 and RUNX1^{R320*} binding site using ChIPSeeker annotation to the hg38 genome for all peaks. Wild-type peaks = 40,679; RUNX1^{R320*} peaks = 38,233. **(C)** Differential binding volcano plot between RUNX1 wild-type and RUNX1^{R320*} ChIP-seq datasets, significantly upregulated binding shown in (red) and downregulated binding (blue) comparing R320*/WT. **(D)** Analysis of gene expression in RUNX1^{R320*} cells relative to RUNX1 WT at genes with RUNX1 promoter binding. **(E)** Enrichment of RUNX1^{R320*} peaks genome-wide using ENCODE K562 annotation data across up, nc (no change), and downregulated binding relative to RUNX1 WT. H3K27ac, H3K4me1, H3K4me3, H3K27me3, and H3K9me3 were used to annotate enhancers, promoters, transcribed regions, repressed regions, and heterochromatin respectively. **(F)** RUNX1 motif presence across enhancers and promoters with up or downregulated binding of RUNX1^{R320*} relative to RUNX1.

Figure 5: GRID-seq reveals extensive remodeling of enhancer-promoter connections in RUNX1R320* cells.

(A) Representative heat map of the GRID-seq dataset detecting RNA association with DNA regions across chromosome 21, only interactions within chromosome 21 are shown. **(B)** Z-score of detected RNA-DNA interactions classified as local, cis, and trans. Local interactions represent nascent RNA interaction with the gene body, cis interactions are within the same chromosome and outside the gene body region, and trans interactions are interchromosomal. **(C)** RNA-DNA interaction density across distance after log transformation demonstrating the power law model of DNA looping and interaction described in Lieberman-Aiden et al. **(D)** Enhancer-promoter interactions identified solely in either RUNX1 wild-type (WT) or RUNX1^{R320*} (R320*) cells or present in both (shared) as detected in GRID-seq. **(E)** Motif analysis of RUNX1^{R320*} regulated enhancer and promoter regions in (D), selected significantly enriched motifs shown. **(F)** Normalized read counts of forkhead box gene expression in K562 RUNX1 wild-type and RUNX1^{R320*} cells via RNA-seq. Each bar represents the mean of three replicates and standard deviation. FOXK1 and FOXK2 subfamilies were measured against the remaining FOX subfamilies using one-way ANOVA. * p ≤ 0.05; ** p ≤ 0.01; *** p ≤ 0.001; **** p ≤ 0.0001

Figure 6: FOXK2 cooperates with RUNX1R320* to regulate MYC.

(A) Analysis of K562 H3K27ac (ENCODE ENCFF465GBD), FOXK2 (ENCODE ENCFF286IOU), RUNX1 wild-type and RUNX1^{R320*} binding at MYC and MYC enhancer regions up and downstream of MYC (top). GRID-seq long-range interaction map of chromatin associated RNAs at the MYC locus (bottom). Interaction strength with a greater score between RUNX1 or RUNX1^{R320*} denoted in blue and red respectively. **(B-C)** CUT&RUN qPCR analysis of FOXK2, RUNX1, and RUNX1^{R320*} at MYC BENC enhancer element 3 'E3'. **(D-E)** Western blots examining FOXK2 and MYC protein levels in wild-type (WT) RUNX1 and RUNX1^{R320*} cells transduced with non-targeting shCtl or FOXK2 shRNAs with β-actin loading control. **(F)** Model describing the role of RUNX1^{R320*} and FOXK2 in MYC enhancer regulation. Student's t-test was used to determine significance: * $p \leq 0.05$; ** $p \leq 0.01$; *** $p \leq 0.001$; **** $p \leq 0.0001$.

Figure 1

Figure 1

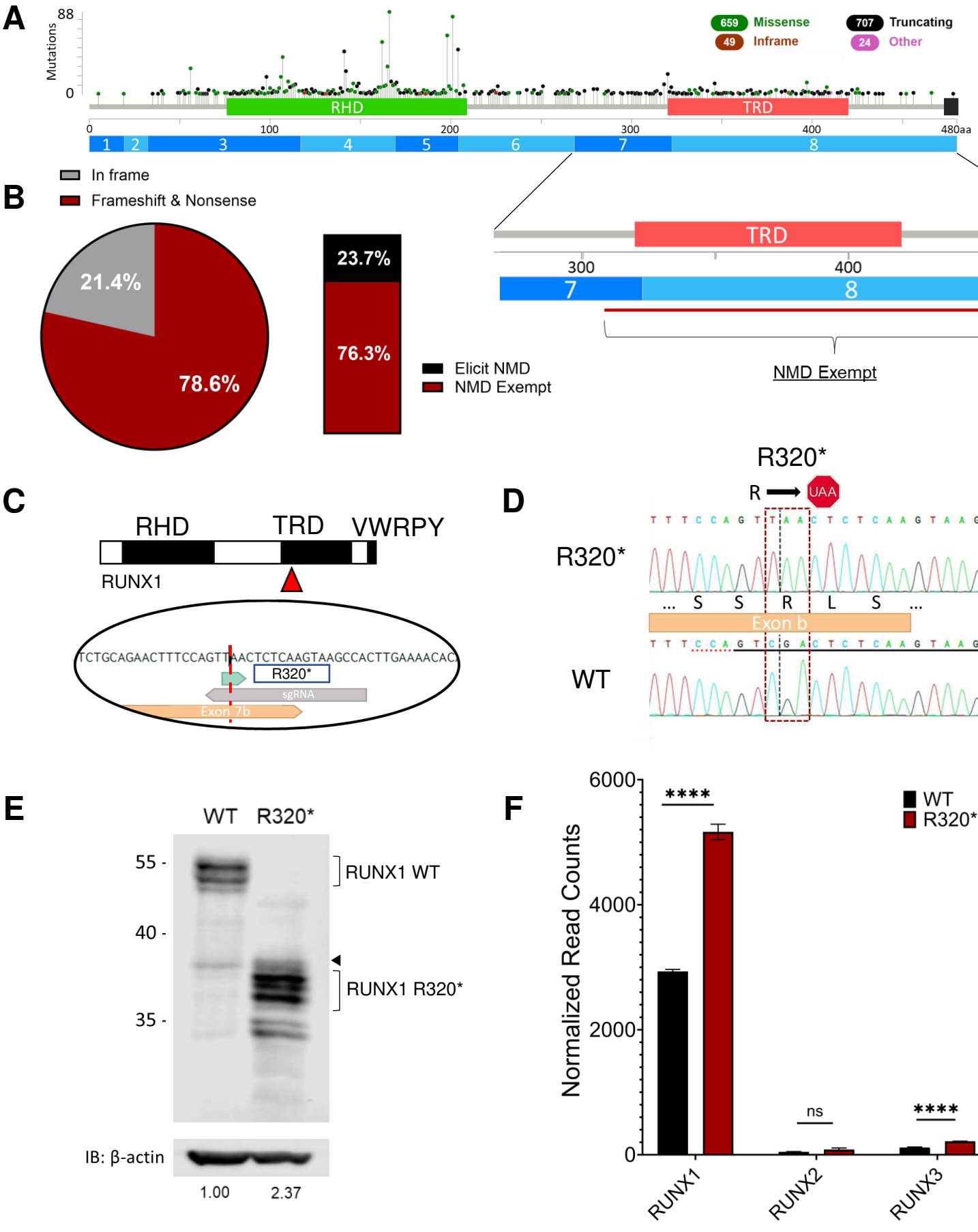

Figure 2

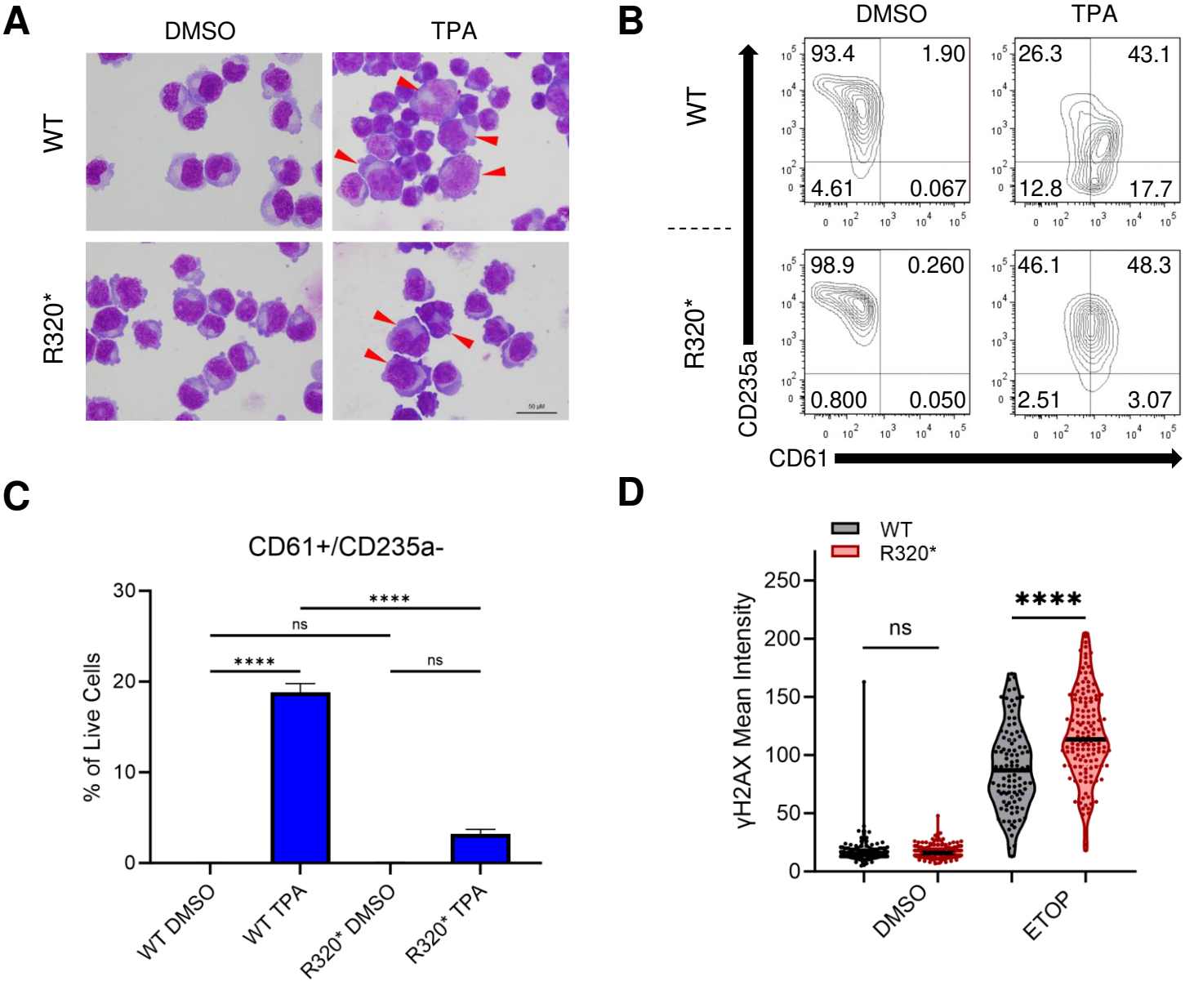

Figure 3

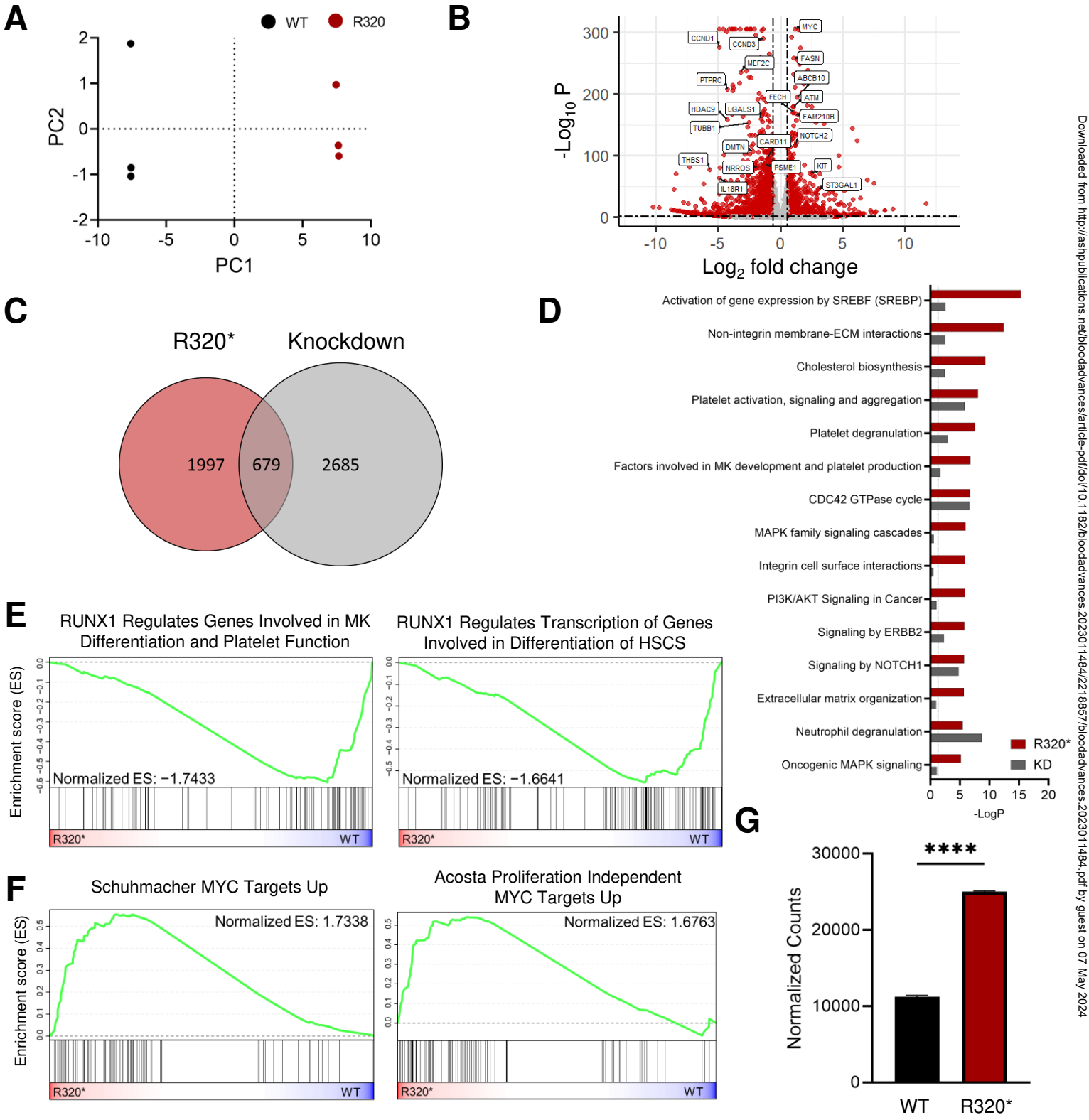

Figure 4

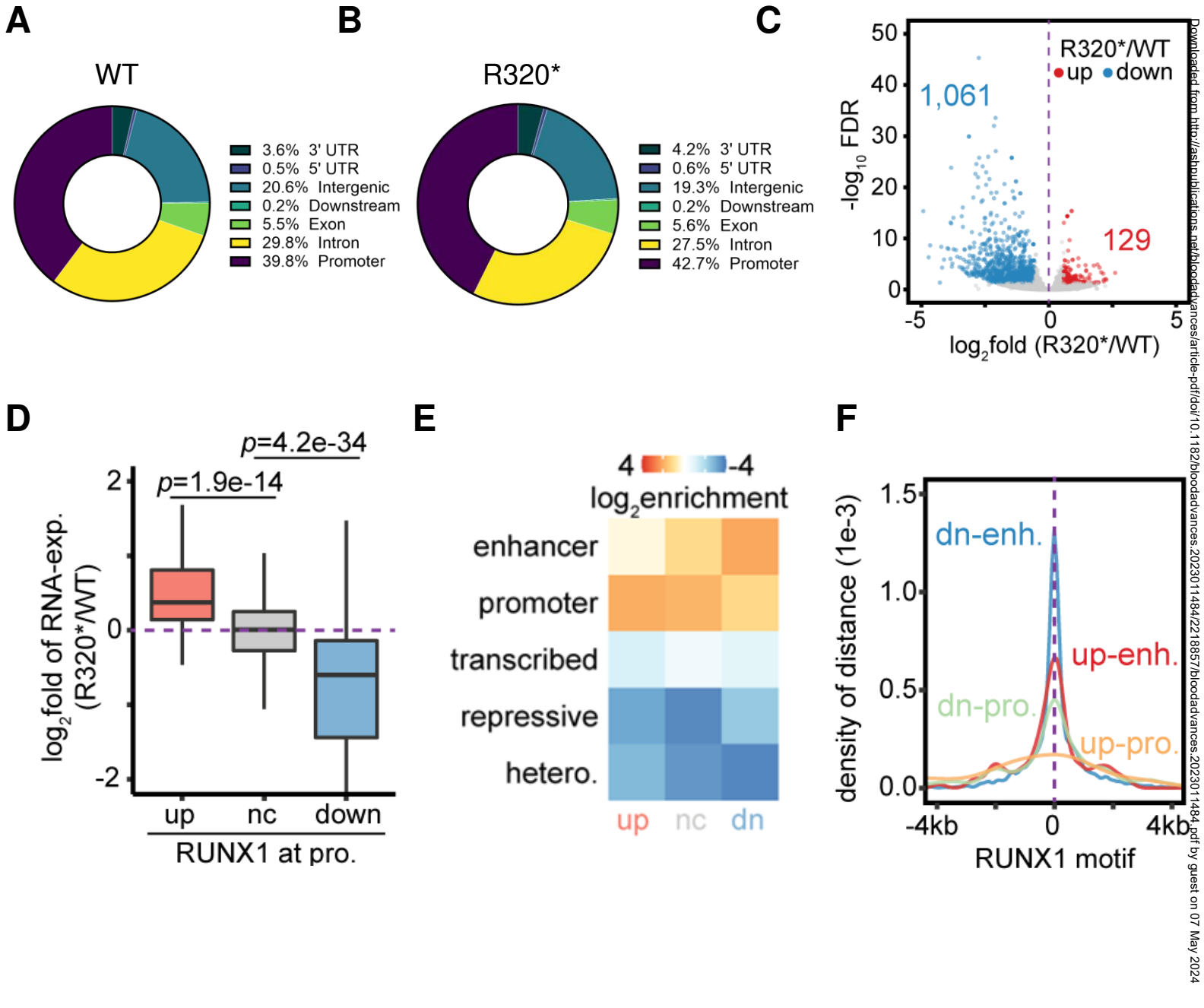

Figure 5

Figure 5

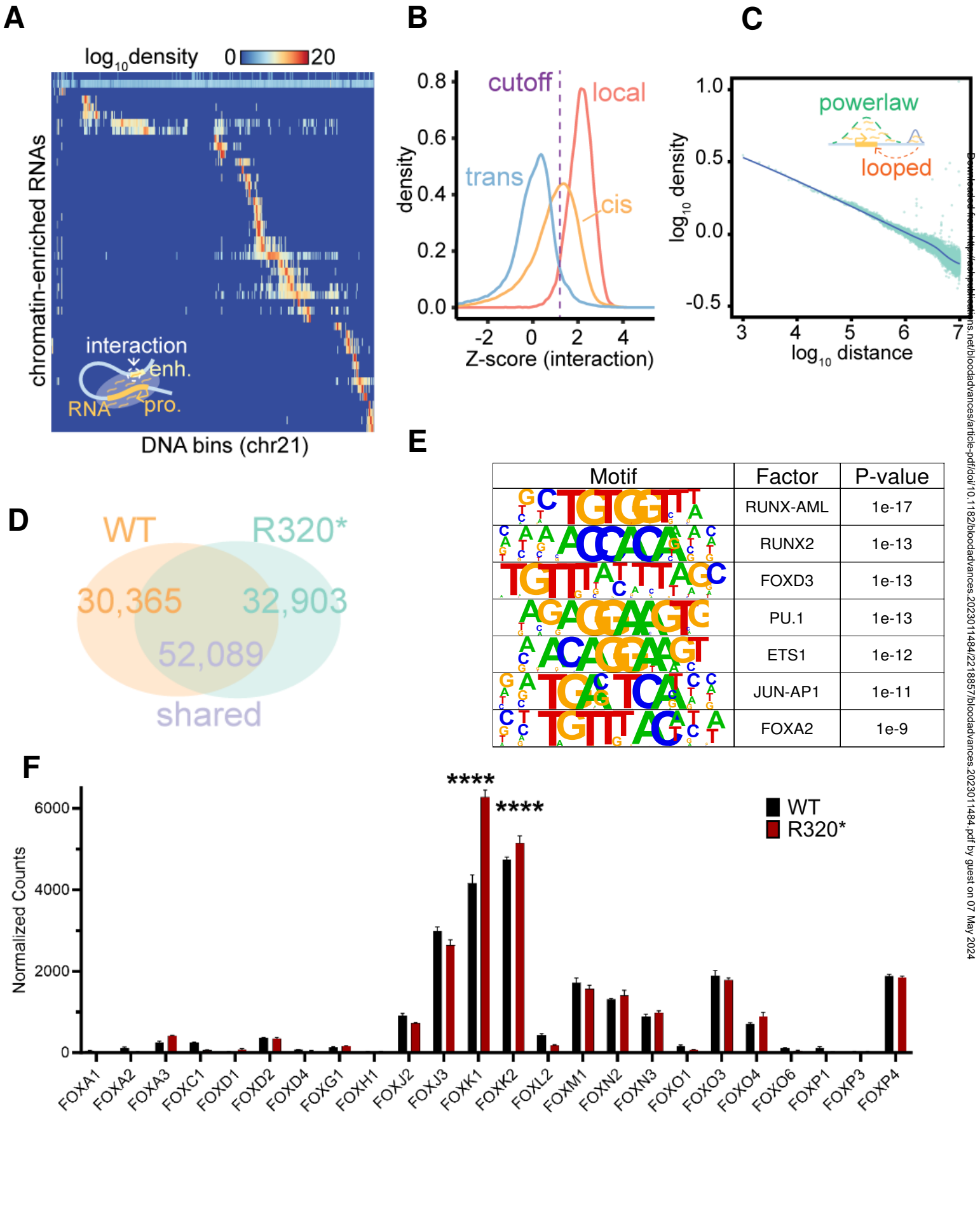

Figure 6